

Relaxation of hot-electron distributions in GaAs

Chang Sub Kim and Bernie Shizgal

Department of Chemistry, University of British Columbia, Vancouver, British Columbia, Canada V6T1Y6
(Received 5 July 1990; revised manuscript received 7 January 1991)

The field-free equilibration of optically excited nonequilibrium hot electrons is studied theoretically with use of the Boltzmann kinetic equation. The analysis is limited to the situation where the longitudinal-optical-phonon scattering mechanism is dominant. The relaxation of the electron-energy-distribution function and of the average electron energy are investigated numerically for pulsed initial conditions with account taken of the exact collision integral within a single-parabolic-band model. It is shown that the energy dependence of the relevant scattering rate plays an important role in determining the relaxation of the hot-electron distribution.

I. INTRODUCTION

There has recently been considerable experimental and theoretical interest in the relaxation of nonequilibrium distributions of hot carriers in semiconductors.¹⁻⁸ Experimental studies have been carried out for optically excited or electrically injected hot carriers in GaAs as well as quantum-well structures such as GaAs/Al_xGa_{1-x}As. With the development of subpicosecond resolution spectroscopy,²⁻⁵ the relaxation phenomena in semiconductors can now be studied experimentally on a very short time regime. The development of such experimental techniques provides further motivation for research on more exact theoretical treatments of relaxation dynamics. It has long been recognized that semiconductor device characteristics depend on the relaxation rates of nonequilibrium distributions.^{9,10} A detailed understanding of the relaxation to a steady state in terms of the various interactions of electrons in a semiconductor and the details of the time variation of the distribution functions is clearly an important endeavor.

The purpose of the present paper is the theoretical study of the field-free relaxation to equilibrium of the nonequilibrium energy distribution of hot electrons injected into GaAs. The importance of this problem has been discussed by Shah¹¹ and Ulbrich¹² in recent reviews of hot-electron transport. We assume that the dominant scattering process for energetic electrons in GaAs is the longitudinal-polar-optical-phonon interaction and that electron-electron collisions can be neglected as discussed by Collins and Yu.¹³ For temperatures above 25 K, acoustic phonon scattering does not play an important role.¹⁴ The main objective is to obtain the time dependence of the electron-energy-distribution function, $f(E,t)$, from a solution of the Boltzmann equation for this interaction without approximating the collision operator. We also calculate the relaxation of the average electron energy and the relaxation time for the approach to equilibrium. A common approximation used in the solution of the Boltzmann equation for this initial-value problem as well as for the steady-state problem in the presence of an electric field is to replace the exact col-

lision operator with an average relaxation time generally assumed to be constant,¹⁵⁻¹⁷ although an energy dependence is sometimes included.¹⁸

Since electron-electron collisions are neglected, the Boltzmann equation is linear in the electron distribution function. The relaxation is therefore completely specified by the linear Boltzmann collision operator and the initial condition. If the initial distribution function is expanded in the eigenfunctions of the collision operator and the spectrum of the collision operator is discrete, then the time dependence of the average electron energy (and other electron properties) can be represented as a sum of exponential terms of the form $\sum_{n=0}^{\infty} c_n e^{-\lambda_n t}$, where λ_n are the eigenvalues of the collision operator and the coefficients c_n fit the initial condition. If the spectrum of the operator is continuous, then the sum over n is replaced by an integral over the continuous eigenvalue λ . These aspects of the approach to equilibrium are well known in their application to gaseous systems¹⁹⁻²¹ and in neutron thermalization processes.^{22,23} The representation in terms of the eigenvalues is useful since if the spectrum is discrete, then the reciprocal of the smallest nonzero eigenvalue is the relaxation time for small departures from equilibrium. This would correspond to the usual relaxation-time approximation often used in dynamical studies in semiconductor physics,^{15,16} but with the identification of the relaxation time with an eigenvalue of the collision operator. The representation of the relaxation in terms of the eigenvalue spectrum of the linear collision operator is not possible with Monte Carlo simulations which have become a common theoretical methodology in recent years.²⁴ If the spectrum of the operator is continuous, then the approach to equilibrium may have a very nonexponential dependence on the time. Such a situation was calculated by Corngold and co-workers²⁵ in the study of energy relaxation in plasmas.

The present work is an extension of the previous treatment of this problem by Canright and Mahan.²⁶ These authors considered a constant relaxation rate independent of the electron energy. Also, Canright and Mahan employed a discrete model for the electron-energy-distribution function which corresponds to electron ve-

locities confined to two dimensions. In the present paper we treat the collision integral exactly for the chosen scattering mechanism, and the energy dependence of the scattering rate is taken into account. The importance of the energy-dependent scattering rate in determining hot-electron transport has been discussed recently by Bernasconi *et al.*²⁷ Canright and Mahan obtained an analytic solution to the discrete Boltzmann equation with a constant scattering rate. The spectrum of the infinite-ordering scattering matrix was found to be completely continuous. Although they showed that the energy dependence of the (discrete) time-varying electron-energy-distribution function, they did not calculate the relaxation of the average electron energy and the characteristic energy relaxation times for the approach to equilibrium, as is done in the present work.

For a detailed quantitative analysis we restrict the physical situation as follows. First, we treat the electrons as nondegenerate for simplicity. The longitudinal-polar-optical-phonon interaction is considered to be the dominant scattering mechanism for energetic carriers in polar semiconductors like GaAs,^{1,11} so that the relaxation of injected hot electrons occurs only via emission and absorption of longitudinal-optical phonons. This simplification may be achieved in a real situation by confining injected electrons within certain energy and concentration ranges at certain background temperatures. Furthermore, we restrict the energy of carriers to be less than 0.3 eV so that intervalley scattering can be neglected and only intraband transitions are considered within a single-parabolic-band model.^{1,25} Although both electrons and holes are excited in principle in the photoexcitation process, we assume that most of the photon energy is assigned to the electrons because the electron effective mass is much smaller than the hole effective mass.²⁸ Finally, the phonons are assumed to be in thermal equilibrium at the lattice temperature so that the distribution function is specified *a priori* as obeying Bose-Einstein statistics, and the phonon energy dispersion is constant. Thus we neglect the possible generation of nonequilibrium phonons.

With these assumptions, we solve the time-dependent Boltzmann equation for a pulsed initial energy distribution, with the rigorous collision operator which includes the exact energy dependence of the scattering rates. Because the phonon energy is assumed to be constant, electrons can be scattered into discrete energy levels equally spaced with one phonon energy $\hbar\omega_0$. Accordingly, the Boltzmann equation itself can be written in a discretized form in energy space, that is, the linear inelastic collision operator is reduced to a finite dimensional matrix. The problem is thus reduced to the determination of the eigenvalues and eigenvectors of the resulting matrix defined in the discretized energy space. The dimensionality of the matrix representative of the linear collision operator is increased until convergence is achieved. The nature of the approach to equilibrium in terms of the eigenvalue spectrum of the inelastic collision operator is discussed briefly. The characteristic energy relaxation times are calculated for lattice temperatures of 77 and 300 K for various initial electron energies.

Canright and Mahan²⁶ obtained an exact analytic solution for the distribution function for a two-dimensional gas model with a constant scattering rate. We have compared our results with those obtained for this model. Our primary result shows that the energy-dependent scattering rate has a significant effect on the dynamics of the injected electron distribution function, the electron-energy relaxation, and the corresponding relaxation time. Collins and Yu¹³ also obtained an analytic solution for the Boltzmann equation with the restriction that $(\partial f / \partial E) \hbar\omega_0 \ll f(E)$.

The paper is organized as follows. In Sec. II the Boltzmann equation for the longitudinal-polar-optical-phonon scattering mechanism is briefly discussed. In Sec. III the calculation of the relaxation of the distribution function based a discretized solution of the Boltzmann equation is outlined. The results and their discussion are given in Sec. IV. A summary of the results is presented in Sec. V.

II. THEORY

The Boltzmann equation appropriate for the description of the evolution of a nondegenerate electron distribution, homogeneous in space and in the absence of external fields, is given by

$$\frac{\partial f(\mathbf{k}, t)}{\partial t} = \int \frac{d\mathbf{k}'}{(2\pi/L)^3} [S(\mathbf{k}, \mathbf{k}')f(\mathbf{k}', t) - S(\mathbf{k}', \mathbf{k})f(\mathbf{k}, t)], \quad (1)$$

where $S(\mathbf{k}, \mathbf{k}')$ is the transition probability of an electron being scattered from the energy state $E_{\mathbf{k}'}$ to $E_{\mathbf{k}}$ per time and L is the size of the semiconductor. The energy-wave-vector relationship $E_{\mathbf{k}}$ is assumed to be $\hbar^2 k^2 / 2m^*$, where m^* is the isotropic electron effective mass within a single-parabolic-band model. The transition rate is specified from the Fermi golden rule:

$$S(\mathbf{k}, \mathbf{k}') = \frac{2\pi}{\pi} |\langle \mathbf{k}' | U | \mathbf{k} \rangle|^2 \delta(E_{\mathbf{k}'} - E_{\mathbf{k}} \pm \hbar\omega_0), \quad (2)$$

where $\pm \hbar\omega_0$ represents emission (+) and absorption (−) of a phonon in the scattering process. For polar-optical-phonon scattering the matrix element of the interaction strength U is given by the Fröhlich formula¹⁵

$$\langle \mathbf{k}' | U | \mathbf{k} \rangle = \left[\frac{e^2 \hbar\omega_0}{2V\epsilon_0} \right]^{1/2} \left[\frac{1}{K_\infty} - \frac{1}{K_0} \right]^{1/2} \frac{1}{|\mathbf{k}' - \mathbf{k}|} \times \begin{cases} \sqrt{n_0} & (\text{absorption}) \\ \sqrt{n_0 + 1} & (\text{emission}) \end{cases}, \quad (3)$$

where e is the electric charge, V is the volume of the crystal, K_∞ and K_0 are the high- and low-frequency dielectric

constants of the medium, and ϵ_0 is the permittivity of free space. Also, the thermal average phonon occupancy n_0 is specified as

$$n_0 = 1 / [\exp(\hbar\omega_0/k_B T_0) - 1],$$

where T_0 is the equilibrium lattice temperature.

With Eqs. (2) and (3) in Eq. (1) and after performing the integration in the Boltzmann equation within the single-parabolic-band model, we find that the collision integral on the right-hand side of Eq. (1) reduces to

$$J(f(E, t)) = \alpha \frac{1}{\sqrt{E}} (n_0 + 1) \ln \left[\frac{\sqrt{E + \hbar\omega_0} + \sqrt{E}}{\sqrt{E + \hbar\omega_0} - \sqrt{E}} \right] f(E + \hbar\omega_0, t) \\ + \alpha \frac{1}{\sqrt{E}} n_0 \ln \left[\frac{\sqrt{E} + \sqrt{E - \hbar\omega_0}}{\sqrt{E} - \sqrt{E - \hbar\omega_0}} \right] f(E - \hbar\omega_0, t) \Theta(E - \hbar\omega_0) - \nu(E) f(E, t), \quad (4)$$

where

$$\alpha = e^2 \omega_0 \sqrt{m^*} (1/K_\infty - 1/K_0) / 4\sqrt{2\pi\hbar\epsilon_0}.$$

In the above, the scattering rate $\nu(E)$ is given by¹⁶

$$\nu(E) \equiv \int \frac{d\mathbf{k}'}{(2\pi/L)^3} S(\mathbf{k}', \mathbf{k}) \\ = \frac{\alpha}{\sqrt{E}} \left[n_0 \ln \left[\frac{\sqrt{E + \hbar\omega_0} + \sqrt{E}}{\sqrt{E + \hbar\omega_0} - \sqrt{E}} \right] + (n_0 + 1) \Theta(E - \hbar\omega_0) \ln \left[\frac{\sqrt{E} + \sqrt{E - \hbar\omega_0}}{\sqrt{E} - \sqrt{E - \hbar\omega_0}} \right] \right], \quad (5)$$

which is the total number of collisions being experienced by an electron in an energy state $E_{\mathbf{k}}$ per unit time. The Heaviside step function Θ in Eqs. (4) and (5) ensures that only electrons with energy larger than one phonon energy can lose energy $\hbar\omega_0$.

Since for this scattering mechanism the electrons lose or gain energy in integer multiples of $\hbar\omega_0$ by emitting or absorbing phonons, we choose the electrons to have the discrete energies

$$E_l = E_0 + l\hbar\omega_0, \quad l = 0, 1, 2, \dots, \quad (6)$$

where E_0 is the excess of the energy of an injected electron measured from the conduction band edge such that $0 \leq E_0 < \hbar\omega_0$. This discretization follows in part from the choice of an initial δ function distribution discussed later. With this choice of discretization, Eq. (1) with the collision integral as in Eq. (4) can be written in the matrix form

$$\frac{\partial f_l(t)}{\partial t} = - \sum_{m=l-1}^{l+1} G_{lm} f_m(t), \quad (7)$$

where $f_l(t) \equiv f(E_l, t)$ and the G_{lm} is given by

$$G = \begin{pmatrix} \nu(E_0) & g_+(E_0) & 0 & 0 & 0 & \dots & 0 \\ g_-(E_1) & \nu(E_1) & g_+(E_1) & 0 & 0 & & 0 \\ 0 & g_-(E_2) & \nu(E_2) & g_+(E_2) & 0 & & 0 \\ 0 & 0 & g_-(E_3) & \nu(E_3) & g_+(E_3) & & 0 \\ 0 & 0 & 0 & \dots & \dots & \dots & \dots \\ 0 & 0 & 0 & 0 & \dots & \dots & \dots \end{pmatrix}. \quad (8)$$

In Eq. (8), $g_+(E_l)$ and $g_-(E_l)$ are the negative of the coefficients of $f(E_{l+1}, t)$ and $f(E_{l-1}, t)$ in Eq. (4), respectively.

The number of electrons and the nonequilibrium average energy are given in terms of the distribution function by

$$N \equiv \sum_{l=0}^{\infty} D(E_l) f_l(t) \quad (9)$$

and

$$\bar{E}(t) \equiv \frac{\sum_{l=0}^{\infty} D(E_l) E_l f_l(t)}{\sum_{l=0}^{\infty} D(E_l) f_l(t)}, \quad (10)$$

where $D(E_l)$ is the factor from the density of states that is

$$(V/2\pi^2)(2m^*/\hbar^2)^{3/2} \sqrt{E_l}.$$

In the work by Canright and Mahan, $D(E_l)$ is taken to be independent of E_l . This restricts the electron velocities to two dimensions in velocity space whereas the treatment in this paper corresponds to the three-dimensional case.

Equation (7) satisfies three basic characteristics of a transport equation that include (a) the detailed balance condition, (b) a Boltzmann distribution at equilibrium, and (c) electron conservation. The detailed balance condition at equilibrium states that

$$\sqrt{E_l} G_{lm} f^{(0)}(E_m) = \sqrt{E_m} G_{ml} f^{(0)}(E_l), \quad m \neq l \quad (11)$$

where $f^{(0)}(E_l)$ is the equilibrium distribution function and T_0 is the background temperature of the phonon bath. The equilibrium solution to Eq. (7) is given by $\sum_{m=l-1}^{l+1} G_{lm} F_m^{(0)} = 0$ and is the Boltzmann distribution function, that is,

$$\frac{f_l^{(0)}}{f_{l-1}^{(0)}} = e^{-\hbar\omega/kT_0}. \quad (12)$$

Since the electron energies are not continuous, Eq. (12) states that the ratio of the distribution function at the chosen energies is given by the Boltzmann factor. This implies that the determinant of the matrix \mathbf{G} , Eq. (8), vanishes; accordingly, there must exist a zero eigenvalue for the matrix whose corresponding eigenvector is the Boltzmann distribution function. Since the total number of injected electrons is preserved in the model considered, we have that

$$\frac{\partial N}{\partial t} = 0. \quad (13)$$

This is clearly seen by multiplying Eq. (7) by the weight factor $D(E_l)$ and performing the sum over E_l , that is,

$$\sum_l D(E_l) J(f(E_l, t)) = 0,$$

where the definition Eq. (9) has been used.

III. CALCULATIONS

In this section we describe the numerical solution of Eq. (7) for a pulsed initial distribution function and the study of the relaxation of the nonequilibrium average electron energy. It is useful to introduce a dimensionless energy E_l^* and dimensionless time t^* by

$$E_l^* \equiv E_l / \hbar\omega_0 = \Delta + l, \quad t^* \equiv \nu_0 t, \quad (14)$$

where $\Delta \equiv E_0 / \hbar\omega_0$ and the characteristic scattering time $\nu_0^{-1} \equiv \alpha / \sqrt{\hbar\omega_0}$. Then in dimensionless form Eq. (7) becomes

$$\frac{\partial f_l(t^*)}{\partial t^*} = - \sum_{m=l-1}^{l+1} G_{lm}^* f_m(t^*), \quad (15)$$

where the distribution function is normalized as in Eq. (9). The tridiagonal matrix elements in Eq. (15) are from Eq. (8)

$$G_{l+1}^* = \frac{n_0 + 1}{\sqrt{\Delta + l}} \ln \left[\frac{\sqrt{\Delta + l + 1} + \sqrt{\Delta + l}}{\sqrt{\Delta + l + 1} - \sqrt{\Delta + l}} \right],$$

$$G_{l-1}^* = - \frac{n_0}{\sqrt{\Delta + l}} \ln \left[\frac{\sqrt{\Delta + l} + \sqrt{\Delta + l - 1}}{\sqrt{\Delta + l} - \sqrt{\Delta + l - 1}} \right] \Theta(l-1), \quad (16)$$

$$G_{ll}^* = - \left[\frac{n_0 + 1}{n_0} G_{ll-1}^* + \frac{n_0}{n_0 + 1} G_{ll+1}^* \right].$$

Hereafter we omit the asterisk for the dimensionless variables. It is useful to symmetrize the nonsymmetric matrix \mathbf{G} , Eq. (16), by defining

$$f_l \equiv E_l^{-1/4} \sqrt{f_l^{(0)}} h_l, \quad (17)$$

such that Eq. (7) becomes

$$\frac{\partial h_l}{\partial t} = - \sum_{m=l-1}^{l+1} M_{lm} h_m, \quad (18)$$

where

$$M_{lm} \equiv \frac{1}{E_l^{-1/4} \sqrt{f_l^{(0)}}} G_{lm} E_m^{-1/4} \sqrt{f_m^{(0)}}. \quad (19)$$

One can show that $M_{lm} = M_{ml}$ using the detailed balance condition, Eq. (11).

We consider a solution to Eq. (18) and hence of Eq. (15) for which the distribution function is expanded in the eigenfunctions of M defined by

$$M_{lm} \psi_m^{(\mu)} = \lambda_\mu \delta_{lm} \psi_m^{(\mu)}, \quad (20)$$

where $\psi_m^{(\mu)}$ denotes the m th component of the μ th eigenvector and λ_μ is the corresponding eigenvalue. The transformation from Eq. (15) to Eq. (18) which symmetrizes the relaxation matrix guarantees that the eigenvalues are real. The solution for the time-dependent distribution function is then given in the form

$$f_l(t) = E_l^{-1/4} \sqrt{f_l^{(0)}} \sum_{\mu=0}^{\infty} b_\mu \exp(-\lambda_\mu t) \psi_l^{(\mu)}, \quad (21)$$

where the constants b_μ are specified from the initial condition. For a pulsed initial condition, when the electrons are injected into a particular energy state E_n , we have the initial distribution

$$f_l(0) = N_0 \delta_{ln}, \quad (22)$$

so that the expansion coefficients b_μ are given by $N_0 E_n^{1/4} \psi_n^{(\mu)} / \sqrt{f_n^{(0)}}$. Thus the distribution function is completely specified by

$$f_l(t) = N_0 \left[\frac{f_l^{(0)}}{f_n^{(0)}} \right]^{1/2} \left[\frac{E_n}{E_l} \right]^{1/4} \times \sum_{\mu=0}^{\infty} \exp(-\lambda_\mu t) \psi_l^{(\mu)} \psi_n^{(\mu)}. \quad (23)$$

The initial condition, Eq. (22), is satisfied since at $t=0$ the completeness relation $\sum_{\mu=0}^{\infty} \psi_l^{(\mu)} \psi_n^{(\mu)} = \delta_{ln}$ gives $f_l(0)$ in Eq. (23).

The calculation of the distribution function given by Eq. (23) reduces to the solution of the eigenvalue problem, Eq. (20), and from practical considerations the order of matrix must be set to some finite value Ω . For the present model, an increase in Ω represents the addition of energy grid points to the end of the energy interval. Since the contributions from the very high energy tail of the distribution function are expected to be negligible, rapid convergence of the solution is anticipated at some finite order for the initial energies considered. We increase the order of matrix Ω until the relative difference of the average energy, calculated from Eq. (10), in two successive time steps approaches arbitrarily close to zero (within 10^{-8}) at each time. The order of the matrix required for convergence with this criterion increases with an increase in the initial energy, and is in the range $15 \leq \Omega \leq 30$ for the initial energies considered. The numerical accuracy was also monitored by checking the conservation of number of particles, Eq. (13).

IV. RESULTS AND DISCUSSION

We have solved the Boltzmann equation with the method described in Sec. III for initial electron energies less than 0.3 eV for temperatures $T_0 = 77$ and 300 K. Since we emphasize the importance of taking into account the exact energy dependence of the collision operator, the scattering rate $\nu(E)$ given by Eq. (5) is shown in Fig. 1. As is seen in Eq. (5), the contribution from absorbing phonons is proportional to the thermal average phonon occupancy n_0 . The value of n_0 is about 0.38×10^{-2} at 77 K so that only the emission of phonons is important at this temperature. On the other hand, at 300 K the occupancy is about 0.31 and the contribution from absorption is not negligible. Thus, at these higher temperatures the relaxation of electrons occurs via both phonon emission and absorption.

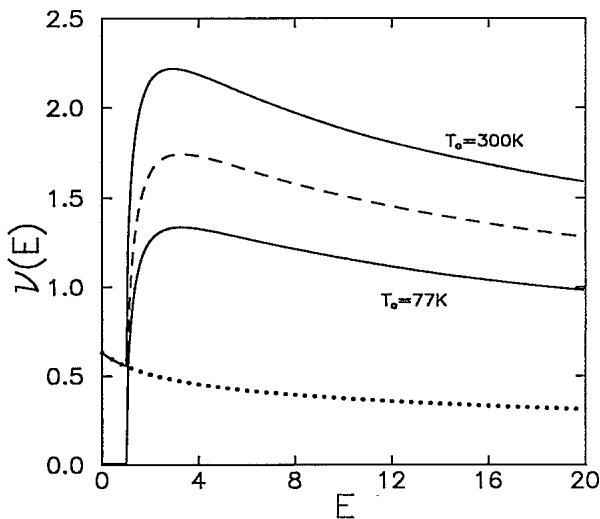


FIG. 1. Scattering rate $\nu(E)$ (in units of $\nu_0 = 0.38 \times 10^{13}$ sec $^{-1}$) vs E (in units of $\hbar\omega_0 = 0.037$ eV); the dashed (dotted) line represents the contribution from emitting (absorbing) phonons for 300 K, respectively. At 77 K, the contribution from absorption is negligible and only the total scattering rate is shown.

To show the relaxation of the distribution functions toward equilibrium, we find it useful to consider the ratio of $f(E_l, t)$ with respect to the equilibrium distribution function, that is,

$$\Phi(E_l, t) \equiv f(E_l, t) / f(E_l, \infty), \quad (24)$$

which tends to unity at long times. In the numerical calculations that were carried out, it was confirmed that

$$f(E_l, t) \rightarrow \exp(-E_l / k_B T_0)$$

as $t \rightarrow \infty$, consistent with Eq. (12). Figure 2 shows the relaxation of the distribution function $\Phi(E_l, t)$ for several temperatures and initial conditions. The times shown are in units of ν_0^{-1} equal to 0.26 picosecond for GaAs.¹⁵ Figures 2(a) and 2(b) are for $T_0 = 77$ K and initial energies $E_3 = 3.1\hbar\omega_0$ and $E_6 = 6.1\hbar\omega_0$, respectively, where the choice $\Delta = 0.1$ has been made in Eq. (14). Figures 2(c) and 2(d) are for $T_0 = 300$ K and initial energies $E_6 = 6.1\hbar\omega_0$ and $E_8 = 8.1\hbar\omega_0$, respectively. A smooth line has been drawn through the data points, although the distribution function is evaluated at the previously defined discrete energy points given by Eq. (14). The initially sharply peaked distribution function at the injected energy broadens with time and approaches the equilibrium Maxwell-Boltzmann distribution at infinite time. The negative portion of the curves indicates an underpopulation of electrons with respect to the equilibrium distribution and the positive part at higher energies represents an overpopulation.

The time dependence of the average electron energy is with Eqs. (10) and (23) given by

$$\bar{E}(t) = \bar{E}_\infty + \sum_{\mu=1}^{\Omega} c_\mu \exp(-\lambda_\mu t), \quad (25)$$

where \bar{E}_∞ is the equilibrium average energy and

$$c_\mu = \sum_{l=0}^{\Omega} E_l \frac{D(E_l)}{D(E_n)} \left[\frac{f_l^{(0)}}{f_n^{(0)}} \right]^{1/2} \left[\frac{E_n}{E_l} \right]^{1/4} \psi_l^{(\mu)} \psi_n^{(\mu)}, \quad (26)$$

and use has been made of the normalization $N \equiv 1$. The relaxation of the average energy corresponding to the distribution functions in Fig. 2 is shown in Fig. 3 which includes several additional initial energies. For $T_0 = 77$ K the average energy after $10t$ is within approximately 8% of its equilibrium value $0.11\hbar\omega_0$ for $n=3$ and about 50% for $n=6$. For $T_0 = 300$ K, the average energy has decayed to within 9% of the equilibrium value $0.87\hbar\omega_0$ and within 1% for $n=6$ and 3, respectively, after $10t$. A comparison of Figs. 2(a) and 2(b) or 2(c) and 2(d) shows that for the larger initial energies, the distribution functions relax to equilibrium slower at both 77 and 300 K as expected than for the smaller initial energies. Also, the distribution function relaxes much faster toward equilibrium at the high temperature for the same initial conditions $n=6$. This is because, as seen in Fig. 1, the electron scattering rate at 300 K is larger than the one at 77 K and the equilibration is faster. Even after $10t$, it is evident from Fig. 2 that there still remains a nonequilibrium hot energy tail in the electron distributions.

In order to characterize the time scale of the energy relaxation, we define an effective time-dependent relaxation time $\tau(t)$ given by

$$\frac{\partial \bar{E}(t)}{\partial t} = -\frac{\bar{E}(t) - \bar{E}_\infty}{\tau(t)}, \quad (27)$$

which with Eqs. (25) and (26) can be written as

$$\tau(t) = \frac{\sum_{\mu=1}^{\Omega} c_{\mu} \exp(-\lambda_{\mu} t)}{\sum_{\mu=1}^{\Omega} c_{\mu} \lambda_{\mu} \exp(-\lambda_{\mu} t)}. \quad (28)$$

The time variation of $\tau(t)$ at $T_0 = 77$ and 300 K and initial conditions $n=6$ and 8 is shown in Fig. 4 and tends to an effective constant relaxation time after some time. The solid and dashed curves are for T_0 equal to 77 and

300 K, respectively. The dotted curve is the result obtained with the model used by Canright and Mahan²⁶ discussed later. For sufficiently long times, it is clear that the relaxation of the average electron energy can be reasonably well characterized by the relaxation-time approximation Eq. (27), with a constant effective relaxation time, which from Eq. (28) would correspond to $1/\lambda_1$. For this case, the electron energy decays to equilibrium exponentially after an initial transient. However, this result requires that the spectrum of the relaxation matrix contain at least one discrete eigenvalue. In general, the eigenvalue spectrum of the matrix Eq. (16) may possess a continuous part as well as discrete values.

In Table I the lowest few eigenvalues of the collision operator Eq. (16) are presented versus the order of the matrix. The zero eigenvalue is the one corresponding to the equilibrium solution, as discussed earlier. The calcu-

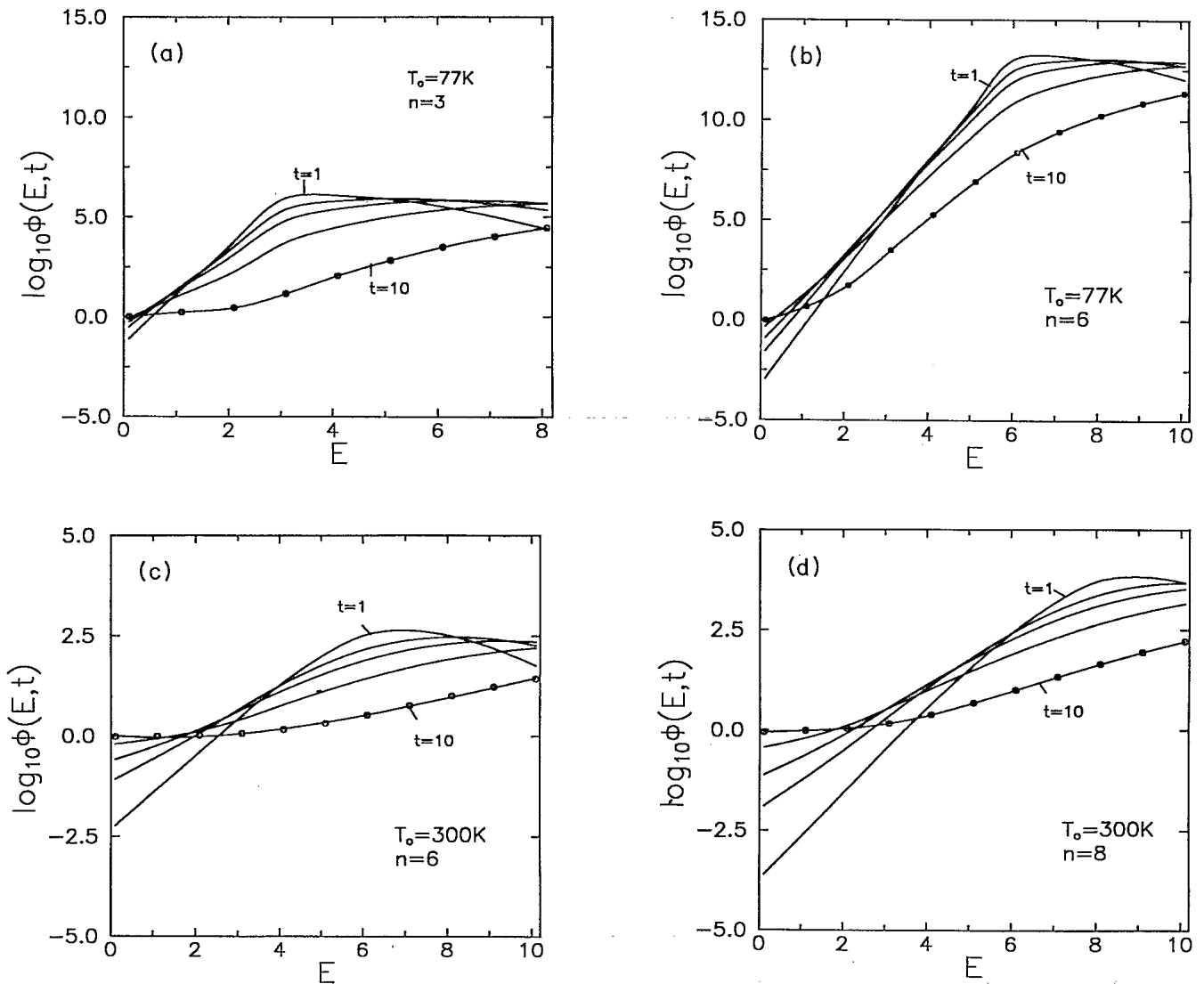


FIG. 2. Relaxation of the distribution functions $\Phi(E, t) \equiv f(E, t)/f(E, \infty)$ for t in units of $\nu_0^{-1} = 0.26$ picosecond equal to 1, 2, 3, 5, and 10. T_0 and the initial peak are equal to (a) 77 K, $n=3$; (b) 77 K, $n=6$; (c) 300 K, $n=6$; (d) 300 K, $n=8$. The symbols (O) indicate the value of the distributions at the discrete energy values.

lations show that at 77 K the spectrum of the relaxation matrix consists of a single nonzero discrete eigenvalue λ_1 plus a continuum, whereas at 300 K the spectrum is entirely continuous. This conclusion is based on the convergence with increasing Ω of the discrete eigenvalue λ_1 at 77 K but the nonconvergence of the eigenvalues which belong to the continuum.

At the lower temperature it is expected that the energy relaxation in the long-time limit is characterized by the single discrete eigenvalue λ_1 . This is seen more clearly in Table II where the values $\lambda_1\tau(t)$ are shown versus time to illustrate the asymptotic behavior of the relaxation time $\tau(t)$. The results in the table show that $\tau(t) \rightarrow 1/\lambda_1$ as $t \rightarrow \infty$ for both $n=6$ and 8 at 77 K. For this case, the long-time limit, Eq. (28), can be rewritten in the form

$$\tau(t) \sim \frac{1}{\lambda_1} + \frac{\int d\lambda C(\lambda) \exp(-\lambda t)}{\int d\lambda C(\lambda) \lambda \exp(-\lambda t)} \text{ as } t \rightarrow \infty, \quad (29)$$

where the coefficient $C(\lambda)$ corresponds to the discrete C_μ

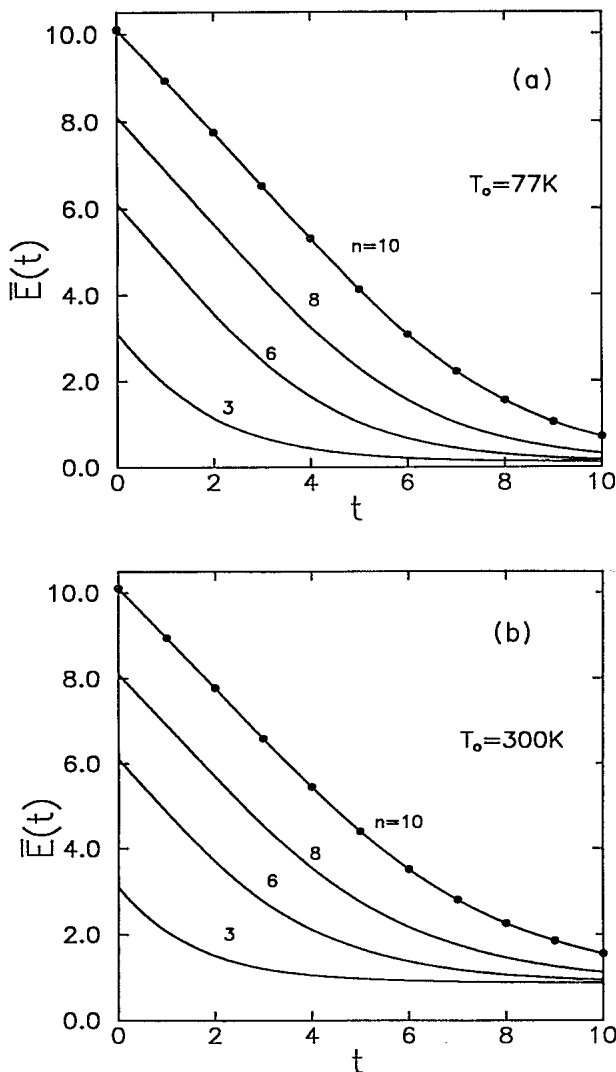


FIG. 3. Decay of the average electron energy $\bar{E}(t)$ at temperatures 77 and 300 K for initial conditions $n=3, 6, 8,$ and 10 .

TABLE I. Convergence of the lower-order eigenvalues vs the order of the matrix Ω .

Ω	λ_0	λ_1	λ_2	λ_3
$T_0=77 \text{ K}$				
5	0.7068[-11] ^a	0.5972	1.193	1.448
10	0.6357[-17]	0.5972	1.149	1.186
15	0.6357[-17]		1.034	1.076
20			0.9473	0.9812
25			0.8823	0.9103
30			0.8313	0.8551
$T_0=300 \text{ K}$				
5	0.3269[-2]	0.8017	1.501	2.571
10	0.3216[-5]	0.5044	0.7533	1.087
15	0.2809[-8]	0.4300	0.5437	0.7134
20	0.2354[-11]	0.3914	0.4598	0.5547
25	0.1710[-14]	0.3632	0.4149	0.4752
30	-0.2457[-15]	0.3408	0.3839	0.4287

^a[- n] $\equiv 10^{-n}$.

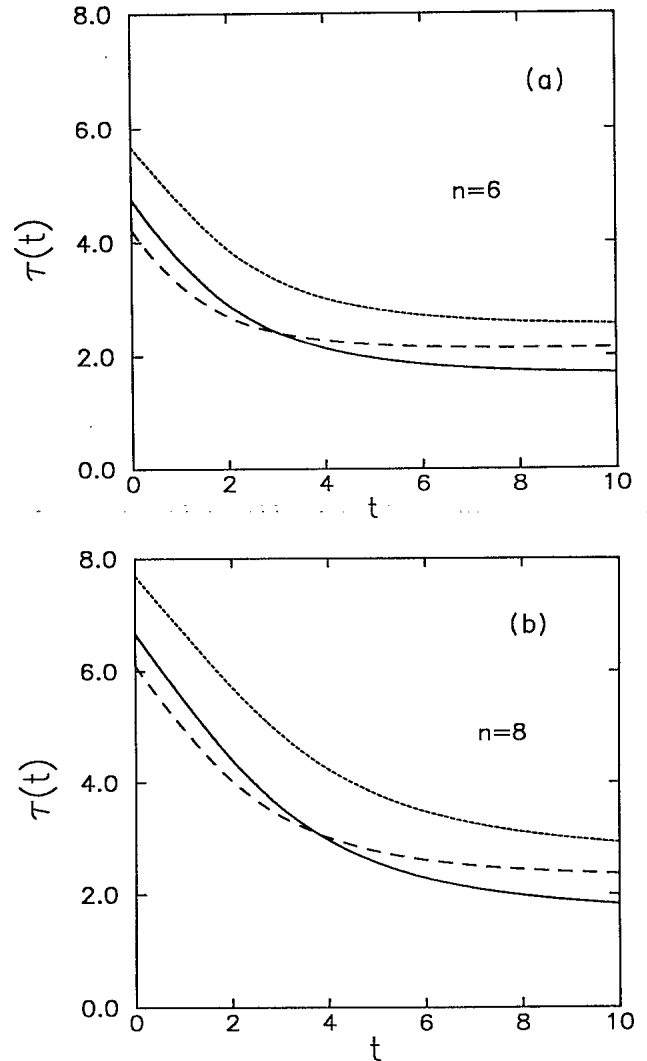


FIG. 4. Time-dependent relaxation time for initial conditions (a) $n=6$ and (b) $n=8$. The solid line is the result from exact energy-dependent theory at 77 K, the dashed line is the same result at 300 K, and the dotted line is the result from the constant scattering rate model at 300 K.

TABLE II. $\lambda_1\tau(t)$ vs t (in units of $\nu_0^{-1}=0.26$ picosecond).

t	77 K, $n=6$	300 K, $n=6$	77 K, $n=8$	300 K, $n=8$
1	2.1997	1.3419	3.2770	1.0775
2	1.7299	1.0893	3.6247	1.5774
3	1.4442	0.9601	2.1272	1.3091
4	1.2751	0.8888	2.7710	1.1410
5	1.1726	0.8458	1.5326	1.0337
6	1.1089	0.8179	1.3706	0.9621
7	1.0686	0.7984	1.2606	0.9121
8	1.0430	0.7842	1.1804	0.8757
9	1.0267	0.7733	1.1301	0.8481
10	1.0164	0.7645	1.0917	0.8266
11	1.0099	0.7571	1.0643	0.8092
12	1.0060	0.7508	1.0448	0.7950
13	1.0035	0.7452	1.0310	0.7830
14	1.0021	0.7401	1.0212	0.7727
15	1.0012	0.7354	1.0144	0.7637

in Eq. (28) and λ_1 is the lowest discrete nonzero eigenvalue. On the other hand, at 300 K the spectrum is entirely continuous and the second integral term contributes so that the time dependence is no longer a pure exponential. The functional form of $C(\lambda)$ versus λ determines the time dependence. It is interesting to speculate as to whether the different time dependence at 77 and 300 K can be observed experimentally. The differences in the results at these two temperatures demonstrates the important role of the energy dependence of the collision operator. The model studied by Canright and Mahan yields a spectrum that is entirely continuous and the energy relaxation is not exponential.

It is useful to characterize the relaxation with a time-independent relaxation time which can be defined in a variety of ways as discussed elsewhere in connection with gaseous systems.^{19-23,25} We choose to define a relaxation time τ_e after which the difference $\bar{E}(\tau_e) - \bar{E}_\infty$ has decreased by the factor e^{-1} of its initial value, that is,

$$\bar{E}(\tau_e) - \bar{E}_\infty = e^{-1} [\bar{E}(0) - \bar{E}_\infty].$$

In Table III we show the relaxation time τ_e for various initial conditions and for temperatures 77 and 300 K. The relaxation times at the higher temperature are smaller for the same initial condition as anticipated.

Also shown in Table III, and in Fig. 4, are the results for the model of Canright and Mahan.²⁶ Canright and

TABLE III. The effective relaxation time.

n	τ_e (77 K) ^a	τ_e (300 K) ^b	τ_e (300 K, const ν)
3	0.504	0.435	0.551
6	0.842	0.790	1.040
8	1.113	1.067	1.363
10	1.409	1.363	1.687

(τ_e in picoseconds).

^aResults obtained with the three-dimensional energy-dependent scattering operator.

^bResults obtained with the two-dimensional energy-independent scattering operator by Canright and Mahan.

Mahan employed a two-dimensional model with a constant scattering rate for which the relaxation matrix Eq. (16) is given by

$$\begin{aligned} G_{ll+1} &= -(n_0 + 1), \\ G_{ll-1} &= -n_0\Theta(l-1), \\ G_{ll} &= [(n_0 + 1)\Theta(l-1) + n_0]. \end{aligned} \quad (30)$$

They showed that, in addition to the zero eigenvalue corresponding to the equilibrium solution, the eigenvalues of the matrix in Eq. (30) form a continuous spectrum $\lambda(\theta)$ parametrized by an angle θ , which varies from $\theta=0$ to $\theta=\pi$. Because of the two-dimensional nature of their model, the particle number density and energy, Eqs. (9) and (10), are given by

$$N \equiv \sum_{l=0}^{\infty} f_l(t), \quad (31)$$

$$\bar{E}(t) \equiv \frac{\sum_{l=0}^{\infty} E_l f_l(t)}{\sum_{l=0}^{\infty} f_l(t)}.$$

A direct comparison of the relaxation of the average energy between the energy-dependent case in this paper and the constant scattering rate model by Canright and Mahan is consequently somewhat inappropriate. In the latter, the average energy at equilibrium is given as

$$\bar{E}(\infty) = E_0 + \frac{\hbar\omega_0}{\exp(\hbar\omega_0/k_B T_0) - 1}. \quad (32)$$

In the high-temperature limit $\hbar\omega_0 \ll k_B T_0$, Eq. (32) approaches its equipartition value $k_B T_0$ appropriate to a system with two translational degrees of freedom, whereas Eq. (10) gives the value of $\frac{3}{2}k_B T_0$ consistent with three translational degrees of freedom. The discrepancy stems from the different weight factors in the definitions for the average energy, Eqs. (31) and (10), constant for the former and $\sqrt{E_l}$ for the latter. The different weight factors are also important in determining the form of the collision operator in connection with the conservation of particle number. However, a comparison of the two models is still appropriate. For example, the phonon modes interacting with two-dimensional carriers such as electrons confined in GaAs/Al_xGa_{1-x}As heterojunctions are considered to be the same as those of bulk GaAs.²⁹

The relaxation equation, Eq. (15), is solved with the matrix elements given by Eq. (30) with the methodology described in Sec. III. In Table IV, we show the convergence of the largest and smallest eigenvalues from the numerical diagonalization of the relaxation matrix, Eq. (19), in comparison with the analytic values from Canright and Mahan at the extreme boundaries of the continuous spectrum. The numerical results are in almost complete agreement with the analytic results for this model.

The relaxation of the electron distribution function for $n=6$ at 300 K obtained with the constant relaxation rate is shown in Fig. 5. The corresponding relaxation of the average electron energy is shown in Fig. 6. A comparison of these results with those in Fig. 2 for our three-dimensional energy-dependent model shows that the re-

TABLE IV. Convergence of the eigenvalues for the constant scattering rate model.

$\Omega =$	20	40	60	80	100	$\lambda(\theta)^a$
$\theta = \pi$	0.3607	0.3475	0.3451	0.3443	0.3439	0.3433
$\theta = \pi$	2.8977	2.9091	2.9113	2.9120	2.9124	2.9130

^aAnalytic values from Canright and Mahan, Ref. 26.

laxation is somewhat slower for the constant scattering model. Also, the relaxation is slower for the higher initial energies. The average energy is more than 50% off from its equilibrium value for $n=6$, and about 5% for $n=3$ after $10t$. The constant scattering rate model underestimates the number of collisions experienced by electrons, since the collision rate has been approximated by $2n_0 + 1$ [the diagonal element in Eq. (30)] and the energy dependence has been neglected [see Eq. (16)]. The value of $2n_0 + 1$ is approximately 1.6 at 300 K and 1.0 at 77 K, respectively. Thus, comparing the results in Fig. 4 with the results in Fig. 2 and in view of the comparisons of τ_e in Table III, this model gives a larger nonequilibrium electron population at higher energies, and the slower relaxation of the distribution functions and of the average electron energy. These results suggest that the energy dependence of the collision operator is important for a quantitative description of the relaxation of hot-electron distributions. In addition, the two-dimensional constant scattering rate model considered by Canright and Mahan does not represent the relaxation mechanism in the bulk material. It might be an appropriate approximation for a two-dimensional electron gas in a homogeneous system.

V. SUMMARY

We have obtained the time-dependent hot-electron distributions in GaAs from solutions of the Boltzmann equation for an initial δ -function distribution function at 77 and 300 K, and studied the relaxation to equilibrium

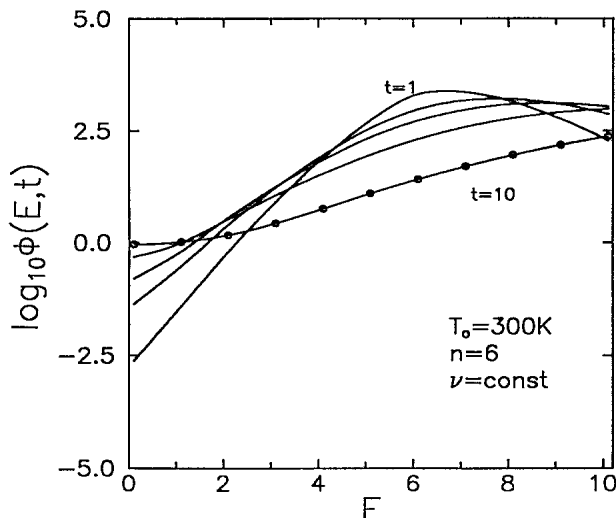


FIG. 5. Relaxation of the distribution functions Φ with $n=6$ at 300 K for the constant scattering rate model.

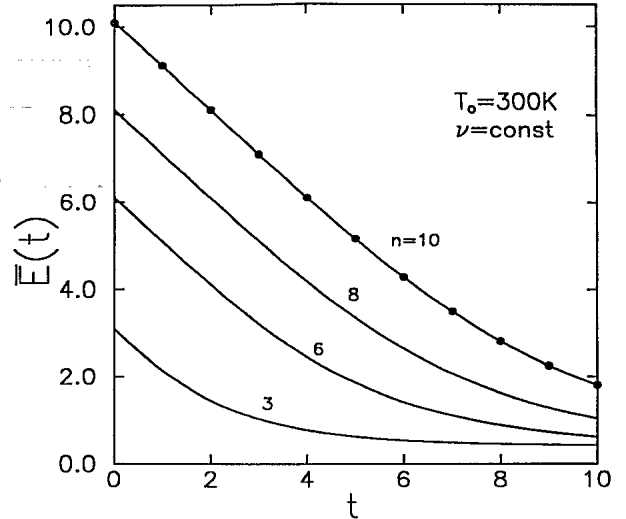


FIG. 6. Decay of the average energy at 300 K for $n=3, 6, 8,$ and 10 .

of the average electron energy. The single-longitudinal-optical-phonon scattering mechanism was assumed and the energy dependence of the scattering rates was rigorously included in the calculations. The solution was expanded in the eigenfunctions of the collision operator determined by the numerical diagonalization of the matrix representative of the collision operator in a discretized energy space.

The nature of the approach of the average energy to equilibrium has been discussed in terms of the eigenvalue spectrum of the collision operator. We find that at 77 K there exists a single discrete nonzero eigenvalue plus a continuum and the asymptotic behavior of the energy relaxation is determined by this discrete eigenvalue. The electron average energy in this case relaxes to equilibrium exponentially with the reciprocal of the discrete nonzero eigenvalue as the asymptotic relaxation time after an initial transient. On the other hand, at 300 K the eigenvalue spectrum is continuous and the approach to equilibrium is some nonexponential function of time.

We have also introduced an effective energy relaxation time in order to characterize the time scale of the energy relaxation for various initial energies and lattice temperatures. The result shows that the average electron energy relaxes faster at the higher temperature than at the lower temperature, and that electrons with high initial energy relax slower for both temperatures. The energy dependence of the scattering rate plays a significant role in the relaxation of injected hot electrons. For the two-dimensional constant scattering rate model by Canright and Mahan,²⁶ the relaxation of the distribution function and of the average energy is somewhat slower. This is because the constant scattering rate model underestimates the number of collisions of electrons in the range of energies considered and yields an incorrect overpopulation of high-energy electrons.

ACKNOWLEDGMENTS

This research is supported by a grant from the Natural Sciences and Engineering Research Council of Canada.

- ¹D. N. Mirlin, I. Ja. Karilik, L. P. Nikitin, I. I. Reshina, and V. F. Sapega, *Solid State Commun.* **37**, 757 (1981).
- ²J. L. Oudar, A. Migus, D. Hulin, G. Grillon, J. Etchepare, and A. Antonetti, *Phys. Rev. Lett.* **53**, 384 (1984); J. L. Oudar, D. Hulin, A. Migus, A. Antonetti, and F. Alexandre, *ibid.* **55**, 2074 (1985).
- ³N. Sawaki, R. A. Höpfel, E. Gornik, and H. Kano, *Appl. Phys. Lett.* **55**, 1996 (1989).
- ⁴J. A. Kash, *Phys. Rev. B* **40**, 3455 (1989).
- ⁵W. H. Knox, C. Hirlimann, D. A. B. Miller, J. Shah, D. S. Chemla, and C. V. Shank, *Phys. Rev. Lett.* **56**, 1191 (1986); W. H. Knox, D. S. Chemla, G. Livescu, J. E. Cunningham, and J. E. Henry, *ibid.* **61**, 1290 (1988).
- ⁶N. Balkan, B. K. Ridley, M. Emeny, and I. Goodridge, *Semicond. Sci. Technol.* **4**, 852 (1989).
- ⁷C. L. Petersen, M. R. Frei, and S. A. Lyon, *Phys. Rev. Lett.* **63**, 2849 (1989).
- ⁸U. Sivan, M. Heiblum, and C. P. Umbach, *Phys. Rev. Lett.* **63**, 992 (1989).
- ⁹H. Kroemer, *Solid-State Electron.* **21**, 61 (1978); S. M. Sze, *Semiconductor Devices, Physics and Technology* (Wiley, New York, 1985).
- ¹⁰*Hot Electron Transport in Semiconductors*, edited by L. Reggiani (Springer-Verlag, New York, 1985).
- ¹¹J. Shah, *Solid-State Electron.* **21**, 43 (1978); see also recent papers in *Hot Carriers in Semiconductors*, Proceedings of the Sixth International Conference, edited by D. K. Ferry and L. A. Akers [*Solid-State Electron.* **32**, 1989].
- ¹²R. G. Ulbrich, *Solid-State Electron.* **21**, 51 (1978); see also recent papers by L. Reggiani and L. Varani, *ibid.* **32**, 1383 (1989); M. Nedjalkov and P. Vitanov, *ibid.* **32**, 893 (1989).
- ¹³C. L. Collins and P. Y. Yu, *Phys. Rev. B* **30**, 4501 (1984).
- ¹⁴S. Das Sarma, J. K. Jain, and R. Jalabert, *Phys. Rev. B* **37**, 1228 (1988).
- ¹⁵K. Seeger, *Semiconductor Physics* (Springer-Verlag, New York, 1989); B. R. Nag, *Theory of Electrical Transport in Semiconductors* (Pergamon, Oxford, 1972).
- ¹⁶N. W. Ashcroft and N. D. Mermin, *Solid State Physics* (Saunders College, Philadelphia, 1976).
- ¹⁷G. D. Mahan, *J. Appl. Phys.* **58**, 2242 (1985); H. U. Baranger and J. W. Wilkins, *Phys. Rev. B* **30**, 7349 (1984).
- ¹⁸J. P. Nougier, J. C. Vaissiere, D. Gasquet, J. Zimmerman, and E. Constant, *J. Appl. Phys.* **52**, 825 (1981).
- ¹⁹M. R. Hoare and C. H. Kaplinsky, *J. Chem. Phys.* **52**, 3336 (1976).
- ²⁰M. R. Hoare, *Adv. Chem. Phys.* **20**, 135 (1971).
- ²¹B. Shizgal and D. A. R. McMahon, *Phys. Rev. A* **32**, 3669 (1985); B. Shizgal, *Can. J. Phys.* **42**, 97 (1984); B. Shizgal and R. Blackmore, *Chem. Phys.* **77**, 417 (1983); R. Blackmore and B. Shizgal, *Can. J. Phys.* **61**, 1038 (1983).
- ²²N. Corngold, P. Michael, and W. Wollman, *Nucl. Sci. Eng.* **15**, 13 (1963).
- ²³H. Risken and K. Voigtlaender, *Z. Phys. B* **54**, 253 (1984).
- ²⁴C. Jacoboni and L. Reggiani, *Rev. Mod. Phys.* **55**, 645 (1983).
- ²⁵N. Corngold, *Phys. Rev. A* **24**, 656 (1981); D. Rollins and N. Corngold, *Phys. Fluids* **30**, 393 (1987); N. Corngold and D. Rollins, *ibid.* **29**, 1042 (1986).
- ²⁶G. S. Canright and G. D. Mahan, *Phys. Rev. B* **36**, 1025 (1987).
- ²⁷J. Bernasconi, E. Cartier, and P. Pfluger, *Phys. Rev. B* **38**, 12567 (1988).
- ²⁸R. Ulbrich, *Phys. Rev. B* **8**, 5719 (1973).
- ²⁹Y. Okuyama and N. Tokuda, *Phys. Rev. B* **40**, 9744 (1989).